3306 *Chem. Mater.* **2009,** *21,* 3306–3314
DOI:10.1021/cm9008305

CHEMISTRY OF MATERIALS
Article

Effective Suppression of Intra- and Interchain Triplet Energy Transfer to Polymer Backbone from the Attached Phosphor for Efficient Polymeric Electrophosphorescence

Kai Zhang,[†] Zhao Chen,[‡] Yang Zou,[†] Shaolong Gong,[†] Chuluo Yang,*[,†] Jingui Qin,[†] and Yong Cao[‡]

[†]*Department of Chemistry, Hubei Key Lab on Organic and Polymeric Optoelectronic Materials, Wuhan University, Wuhan 430072, People's Republic of China, and* [‡]*Institute of Polymer Optoelectronic Materials and Devices, South China University of Technology, Guangzhou 510640, People's Republic of China*

Received March 25, 2009. Revised Manuscript Received June 10, 2009

To systematically investigate the relationship between polymeric electrophosphorescence and polymer structures, we designed and synthesized a series of copolymers with red-emitting iridium complex [$(piq)_2$Irdbm] (where piq is 1-phenylisoquinolin and dbm is dibenzoylmethane) embedded onto the polymer backbone with different chain configurations. We found that triplet energy back transfer from an attached phosphor to polymer backbone can be suppressed not only by enhancing the triplet energy (E_T) of polymer backbone, but also by introducing a sterically hindered units on the backbone. Together with the improved charge transporting ability, high device efficiency can be achieved. A maximum external quantum efficiency of 2.93% with an emission peak of 629 nm is attained from the copolymer PFOxdIrpiq3 with fluorene-*alt*-oxadiazole backbone due to its relative high E_T (2.32 eV). The efficiency is further enhanced to 3.21% under the identical device configuration for the copolymer PFSFIrpiq3 with fluorene-*alt*-spirobifluorene backbone regardless of its relative low E_T (2.18 eV). The promoted efficiency can be attributed to the effective inhibition of interchain triplet energy transfer because of sterically hindered spirobifluorene units on the backbone. The observation suggests a new design principle for electrophosphorescent polymers to suppress the triplet energy transfer to the polymer main chain from the attached phosphor.

Introduction

Phosphorescent heavy metal complexes as emitters in organic light-emitting diodes (OLEDs) have attracted great attention because the strong spin−orbit coupling leads to relatively shorter triplet lifetime, which allows full utilization of both singlet and triplet excitons to obtain 100% internal quantum efficiency in theory for electroluminescence device.[1] High-efficiency OLEDs and polymer light-emitting diodes (PLEDs) have been achieved by doping phosphorescent dyes in either small-molecule host[2] or polymer matrix.[3] However, the blending system may intrinsically suffer from the limitation of efficiency and stability because of the possible energy loss by energy transfer from host to low-lying triplet states, aggregation of dopants even at low-doping concentrations, and potential phase separation. Recently, the PLEDs directly using a single electrophosphorescent polymer have been developed and proven to be an efficient strategy to get rid of phase separation and concentration quenching; however, there is still the problem of triplet energy back transfer from the incorporating heavy metal complexes to

*Corresponding author. E-mail: clyang@whu.edu.cn.

(1) (a) Baldo, M. A.; O'Brien, D. F.; You, Y.; Shoustikov, A.; Sibley, S.; Thompson, M. E.; Forrest, S. R. *Nature* **1998**, *395*, 151. (b) Cao, Y.; Parker, I. D.; Heeger, A. J. *Nature* **1999**, *397*, 414. (c) Wohlgenannt, M.; Tandon, K.; Mazumdar, S.; Ramasesha, S.; Vardeny, Z. V. *Nature* **2001**, *409*, 494. (d) Baldo, M. A.; Lamansky, S.; Burrows, P. E.; Thompson, M. E.; Forrest, S. R. *Appl. Phys. Lett.* **1999**, *75*, 4. (e) Adachi, C.; Baldo, M. A.; Forrest, S. R.; Thompson, M. E. *Appl. Phys. Lett.* **2000**, *77*, 904. (f) Su, Y. J.; Huang, H. L.; Li, C. L.; Chien, C. H.; Tao, Y. T.; Chou, P. T.; Datta, S.; Liu, R. S. *Adv. Mater.* **2003**, *15*, 884. (g) Yeh, S. J.; Wu, M. F.; Chen, C. T.; Song, Y. H.; Chi, Y.; Ho, M. H.; Hsu, S. F.; Chen, C. H. *Adv. Mater.* **2005**, *17*, 285. (h) Rehmann, N.; Ulbricht, C.; Köhnen, A.; Zacharias, P.; Gather, M. C.; Hertel, D.; Holder, E.; Meerholz, K.; Schubert, U. S. *Adv. Mater.* **2008**, *20*, 129. (i) Yang, X.; Müller, D. C.; Neher, D.; Meerholz, K. *Adv. Mater.* **2006**, *18*, 948. (j) Yang, X.; Neher, D. Organic Light Emitting Devices; Müllen, K., Scherf, U., Eds.; Wiley-VCH: Weinheim, Germany, 2006; pp 333−367.

(2) (a) Ikai, M.; Tokito, S.; Sakamoto, Y.; Suzuki, T.; Taga, Y. *Appl. Phys. Lett.* **2001**, *79*, 156. (b) Lamansky, S.; Djurovich, P.; Murphy, D.; Abdel-Razzaq, F.; Lee, H. E.; Adachi, C.; Buttows, P. E.; Forrest, S. R.; Thompson, M. E. *J. Am. Chem. Soc.* **2001**, *123*, 4304. (c) Nazeeruddin, M. K.; Humphry-Baker, R.; Berner, D.; Rivier, S.; Zuppiroli, L.; Graetzel, M. *J. Am. Chem. Soc.* **2003**, *125*, 8790. (d) Yang, C.; Zhang, X.; You, H.; Zhu, L. Y.; Chen, L.; Zhu, L. N.; Tao, Y. T.; Ma, D. G.; Shuai, Z.; Qin, J. *Adv. Funct. Mater.* **2007**, *17*, 651. (e) Zhou, G.; Wong, W. Y.; Yao, B.; Xie, Z.; Wang, L. *Angew. Chem., Int. Ed.* **2007**, *46*, 1149. (f) Ge, Z.; Hayakawa, T.; Ando, S.; Ueda, M.; Akiike, T.; Miyamoto, H.; Kajita, T.; Kakimoto, M. *Adv. Funct. Mater.* **2008**, *18*, 584. (g) Tao, Y.; Wang, Q.; Yang, C.; Wang, Q.; Zhang, Z.; Zou, T.; Qin, J.; Ma, D. *Angew. Chem., Int. Ed.* **2008**, *47*, 8102.

(3) (a) Gong, X.; Robinson, M. R.; Ostrowski, J. C.; Moses, D.; Bazan, G. C.; Heeger, A. J. *Adv. Mater.* **2002**, *14*, 581. (b) Jiang, C. Y.; Yang, W.; Peng, J. B.; Xiao, S.; Cao, Y. *Adv. Mater.* **2004**, *16*, 537. (c) Wu, F. I.; Su, H. J.; Shu, C. F.; Luo, L.; Diau, W. G.; Cheng, C. H.; Duan, J. P.; Lee, G. H. *J. Mater. Chem.* **2005**, *15*, 1035. (d) Niu, Y. H.; Tung, Y. L.; Chi, Y.; Shu, C. F.; Kim, J. H.; Chen, B.; Luo, J.; Carty, A. J.; Jen, A. K. Y. *Chem. Mater.* **2005**, *17*, 3532. (e) Zhang, K.; Chen, Z.; Yang, C.; Zhang, X.; Tao, Y.; Duan, L.; Chen, L.; Zhu, L.; Qin, J.; Cao, Y. *J. Mater. Chem.* **2007**, *17*, 3451.

 Published on Web 07/06/2009

the polymer backbone like in the blending system, which cause a significantly decrease of the device efficiency.[4]

For a blending system, two strategies have been developed to suppress the triplet energy transfer from the phosphor back to the polymer host. Chen et al. designed a series of CBP-based copolymers and demonstrated that the high triplet energy copolymer P(^{t}Bu-CBP) (2.53 eV) as host give better performance than its analogous copolymers with lower triplet energy, because of an decreasing back transfer of triplet energy from the dopant to the host.[5] On the other hand, Chen et al. also demonstrated that an effective shielding of triplet energy transfer from a high E_T phosphor guest to a low E_T polymer host is possible upon introducing dense side chains to the polymer to block direct contact from the guest such that the possibility of Dexter energy transfer between them is reduced to a minimum.[6]

For a single phosphorescent polymer, there are few reports on the inhibition of triplet energy back transfer from the phosphor to the polymer backbone. Holmes and co-workers reported a series of phosphorescent copolymers with red-emitting iridium complexes attached either directly (spacerless) or through an octamethylene-tethered linkage at the 9-position of a 9-octylfluorene host.[7] The photo- and electroluminescence efficiencies of the octamethylene-tethered copolymer are approximately double those of the spacerless copolymer. An external quantum efficiency of 2.0% ph/el at 100 cd/m^2 was achieved for the octamethylene-tethered copolymer. They proposed that the triplet energy back transfer reduces the triplet population at the iridium complexes for the spacerless systems, and could be inhibited by the distance imposed through the tether; Holdcroft et al. found that increasing the triplet energy of the conjugated backbone by incorporation of a 3,4-linked thienyl group raises the energy of the triplet state of the polymer, thereby decreasing triplet energy back transfer from the phosphorescent emitter to the nonemitting polymer backbone.[8]

We previously reported the phosphorescent copolymers with red-emitting iridium complex embedded on the main chains of polyfluorene (PFH) via ancillary β-diketone ligand, which achieved fair device performance with maximum external quantum efficiency of 0.74%.[9] To systematically investigate the relationship between device performance and polymer structures, and thus improve the device efficiency, we herein designed a series of copolymers with red-emitting iridium complex embedded on the polymer backbone with different chain configurations. We demonstrate that triplet energy back transfer from an attached phosphor to polymer backbone can be suppressed not only by enhancing the E_T of polymer backbone but also by introducing a steric hindered units on the backbone. Together with the improved charge transporting ability, high device efficiencies can be achieved. A maximum external quantum efficiencies of 2.93% is attained from the copolymer PFOxdIrpiq3 with fluorene-*alt*-oxadiazole backbone because of the relatively high E_T of the copolymer. The efficiency is further enhanced to 3.21% for the copolymer PFSFIrpiq3 with fluorene-*alt*-spirobifluorene backbone despite its relative low E_T. The promoted efficiency can be attributed to the sterically hindered spirobifluorene units on the backbone, which effective inhibits the interchain triplet energy transfer. The thermal, electrochemical, photophysical and electroluminescent properties of the copolymers will be discussed.

Experimental Section

General Information. ^{1}H NMR and ^{13}C NMR spectra were measured on Varian Unity 300 MHz spectrometer using $CDCl_3$ as solvent. Elemental analyses of carbon, hydrogen, and nitrogen were performed on a Vario EL-III microanalyzer. The molecular weights of the polymers were determined by Agilent 1100 GPC in THF. The number-average and weight-average molecular weights were estimated by using a calibration curve of polystyrene standards. Differential scanning calorimetry (DSC) was performed on a NETZSCH DSC 200 PC unit at a heating rate of 10 °C min^{-1} from 30 to 300 °C under argon. Thermogravimetric analysis (TGA) was undertaken with a NETZSCH STA 449C instrument. The thermal stability of the samples under a nitrogen atmosphere was determined by measuring their weight loss while heating at a rate of 20 °C min^{-1} from 25 to 600 °C. Polymers were dissolved in toluene (1 mg/mL) for films casting. Films were spin-cast on quartz slides at 1500 rpm for 60 s. UV−vis absorption spectra were recorded on Shimadzu UV-2550 spectrophotometer. PL spectra were recorded on Hitachi F-4500 fluorescence spectrophotometer. The PL quantum yields were measured in film state with polyfluorene as reference by an absolute method using the Edinburgh Instruments integrating sphere excited with Xe lamp. The PL lifetimes were measured by a single photon counting spectrometer from Edinburgh Instruments (FLS920) with a hydrogen-filled pulse lamp as the excitation source. The data were analyzed by iterative convolution of the luminescence decay profile with the instrument response function using the software package provided by Edinburgh Instruments. Cyclic voltammetry (CV) was carried out on a CHI voltammetric analyzer at room temperature in nitrogen-purged anhydrous acetonitrile with tetrabutylammonium hexafluorophosphate ($TBAPF_6$) as the supporting electrolyte at scanning rate of 100 mV/s. A platinum disk and a silver wire were used as working electrode and quasi-referenced electrode, respectively. Polymers are dropped on the platinum disk as film from chloroform solution. Ferrocene was used for potential calibration. The onset potential was determined from the intersection of two tangents drawn at the rising and background current of the cyclic voltammogram.

(4) (a) Sudhakar, M.; Djurovich, P. I.; Hogen-Esch, T. E.; Thompson, M. E. *J. Am. Chem. Soc.* **2003**, *125*, 7796. (b) Sandee, A. J.; Williams, C. K.; Evans, N. R.; Davies, J. E.; Boothby, C. E.; Köhler, A.; Friend, R. H.; Holmes, A. B. *J. Am. Chem. Soc.* **2004**, *126*, 7041.
(5) Chen, Y. C.; Huang, G. S.; Hsiao, C. C.; Chen, S. A. *J. Am. Chem. Soc.* **2006**, *128*, 8549.
(6) Huang, S. P.; Jen, T. H.; Chen, Y. C.; Hsiao, A. E.; Yin, S. H.; Chen, H. Y.; Chen, S. A. *J. Am. Chem. Soc.* **2008**, *130*, 4699.
(7) Evans, N. R.; Devi, L. S.; Mak, C. S. K.; Watkins, S. E.; Pascu, S. I.; Köhler, A.; Friend, R. H.; Williams, C. K.; Holmes, A. B. *J. Am. Chem. Soc.* **2006**, *128*, 6647.
(8) Schulz, G. L.; Chen, X.; Chen, S. A.; Holdcroft, S. *Macromolecules* **2006**, *39*, 9157.
(9) Zhang, K.; Chen, Z.; Yang, C.; Zou, Y.; Gong, S.; Qin, J.; Cao, Y. *J. Phys. Chem. C.* **2008**, *112*, 3907.

Scheme 1. Synthesis of the Monomers

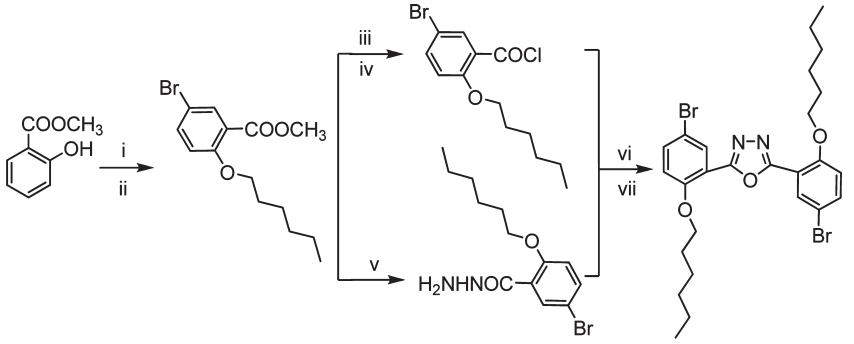

i, $Br_2/FeCl_3$, CH_2Cl_2; ii, $C_6H_{13}Br/K_2CO_3$, DMF; iii, $NaOH/H_2O$; iv, $SOCl_2$; v, $NH_2NH_2{\cdot}H_2O/MeOH$; vi, NEt_3/DMF; vii, $POCl_3$.

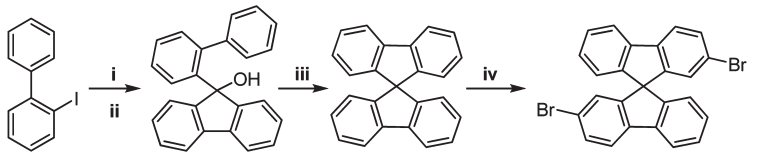

i, Mg, THF; ii, Fluorenone; iii, AcOH/HCl; iv, $Br_2/FeCl_3$, CH_2Cl_2.

All reagents commercial available were used as received unless otherwise stated. The solvents (THF, toluene) were purified by routine procedure and distilled under dry argon before using. All reactions were carried out using Schlenk techniques in an argon atmosphere. 9,9-Dihexylfluorene-2,7-bis(trimethyleneborate) was purchased from Aldrich. 2,2'-dibromo-9,9'-spirobifluorene,[10] 2,5-bis-(5-bromo-2-hexyloxy-phenyl)-[1,3,4]oxadiazole,[11] (1-phenylisoquinoline)$_2$Ir(dibenzoylmethane) ((piq)$_2$Irdbm), (1-phenylisoquinoline)$_2$Ir[1,3-bis(*p*-bromophenyl)-1,3-propanedione] ((piq)$_2$IrdbmBr), PFH, PFHIrpiq3,[9] PFCz, and PFCzIrpiq3[12] were prepared according to the published procedure.

PFSF. A mixture of 9,9-dihexylfluorene-2,7-bis(trimethyleneborate) (0.15 g, 0.3 mmol), 2,2′-dibromo-9,9′-spirobifluorene (0.143 g, 0.3 mmol), Pd(PPh$_3$)$_4$ (10 mg, 3% mmol), and Bu_4NOH (5 mL, 10% aqueous solution) in 5 mL of toluene in a Schlenk tube was stirred at 100 °C for 72 h. After reaction, the resulting polymers were purified by precipitated in methanol twice and washed with acetone in a Soxhlet apparatus for 72 h. Yield: 80%. ^{1}H NMR (300 MHz, $CDCl_3$, δ): 7.92−7.89, 7.69, 7.52, 7.38, 7.12−7.08, 6.97, 6.88, 6.78, 1.85, 1.59, 0.92, 0.66−0.54. M_n: 16920. PDI: 2.19.

PFSFIrpiq3. A mixture of (piq)$_2$IrdbmBr (18 mg, 0.018 mmol), 9,9-dihexylfluorene-2,7-bis-(trimethyleneborate) (0.15 g, 0.3 mmol), 2,2′-dibromo-9,9′-spirobifluorene (0.134 g, 0.282 mmol), Pd(PPh$_3$)$_4$ (10 mg, 3% mmol), and Bu_4NOH (5 mL, 10% aqueous solution) in 5 mL of toluene in a Schlenk tube was stirred at 100 °C for 72 h. After reaction, the resulting polymers were purified by precipitation in methanol twice and washed with acetone in a Soxhlet apparatus for 72 h. Yield: 83%. ^{1}H NMR (300 MHz, $CDCl_3$, δ): 7.96−7.88, 7.69, 7.53, 7.40, 7.13−7.10, 6.99, 6.89−6.87, 6.79−6.77, 1.91, 1.59, 0.95, 0.68−0.55. ^{13}C NMR (75 MHz, $CDCl_3$, δ): 151.79, 150.07, 149.54, 141.69, 141.27, 140.16, 139.89, 128.09, 127.39, 126.31, 124.43, 122.90, 121.41, 120.52, 120.29, 119.97, 55.47, 40.41, 31.51, 29.70, 23.81, 22.68, 14.18.

PFOxd. A mixture of 9,9-dihexylfluorene-2,7-bis(trimethyleneborate) (0.15 g, 0.3 mmol), 2,5-bis-(5-bromo-2-hexyloxy-phenyl)-[1,3,4]oxadiazole (0.184 g, 0.3 mmol), Pd(PPh$_3$)$_4$ (10 mg, 3% mmol) and Bu_4NOH (5 mL, 10% aqueous solution) in 5 mL of toluene in a Schlenk tube was stirred at 100 °C for 72 h. After reaction, the resulting polymers were purified by precipitated in methanol twice and washed with acetone in a Soxhlet apparatus for 72 h. Yield: 90%. ^{1}H NMR (300 MHz, $CDCl_3$, δ): 8.36, 7.81−7.77, 7.63−7.59, 7.18−7.15, 4.20−4.12, 2.07, 1.91−1.85, 1.62, 1.50, 1.23−1.17, 1.07, 0.81−0.72. M_n: 13610. PDI: 1.99.

PFOxdIrpiq3. A mixture of (piq)$_2$IrdbmBr (18 mg, 0.018 mmol), 9,9-dihexylfluorene-2,7-bis- (trimethyleneborate) (0.15 g, 0.3 mmol), 2,5-bis-(5-bromo-2-hexyloxy-phenyl)-[1,3,4]oxadiazole (0.163 g, 0.282 mmol), Pd(PPh$_3$)$_4$ (10 mg, 3% mmol), and Bu_4NOH (5 mL, 10% aqueous solution) in 5 mL of toluene in a Schlenk tube was stirred at 100 °C for 72 h. After reaction, the resulting polymers were purified by precipitation in methanol twice and washed with acetone in a Soxhlet apparatus for 72 h. Yield: 83%. ^{1}H NMR (300 MHz, $CDCl_3$, δ): 8.36, 7.97, 7.63−7.59, 7.18−7.15, 4.18−4.14, 2.07, 1.91−1.87, 1.65, 1.51−1.48, 1.26−1.23, 1.07, 0.77−0.74. ^{13}C NMR (75 MHz, $CDCl_3$, δ): 163.95, 157.10, 152.05, 140.20, 138.87, 134.51, 131.68, 129.32, 125.95, 121.28, 120.30, 114.27, 113.56, 69.44, 55.66, 40.79, 31.76, 29.98, 29.47, 25.92, 24.09, 22.87, 22.75, 14.25.

Fabrication and Measurement of PLED Devices. Polymers were dissolved in *p*-xylene and filtered with a 0.45 μm filter. Patterned ITO-coated glass substrates were cleaned with acetone, detergent, distilled water, and 2-propanol, subsequently, in an ultrasonic bath. After treatment with oxygen plasma, 150 nm of poly(3, 4-ethylenedioxythiophene) (PEDOT) doped with poly(styrenesulfonic acid) (PSS) (Batron-p 4083, Bayer AG) was spin-coated onto the ITO substrate followed by drying in a vacuum oven at 80 °C for 8 h. A thin film of polymers was coated onto the anode by spin-casting inside drybox. The film thickness of the active layers was around 75−80 nm, measured with an

(10) Pei, J.; Ni, J.; Zhou, X.; Cao, X.; Lai, Y. *J. Org. Chem.* **2002**, *67*, 4924.
(11) Song, S. Y.; Ahn, T.; Shim, H. K.; Song, I. S.; Kim, W. H. *Polymer* **2001**, *42*, 4803.
(12) Zhang, K.; Chen, Z.; Yang, C.; Gong, S.; Qin, J.; Cao, Y. *Macromol. Rapid Commun.* **2006**, *27*, 1926.

Scheme 2. Synthesis of the Copolymers

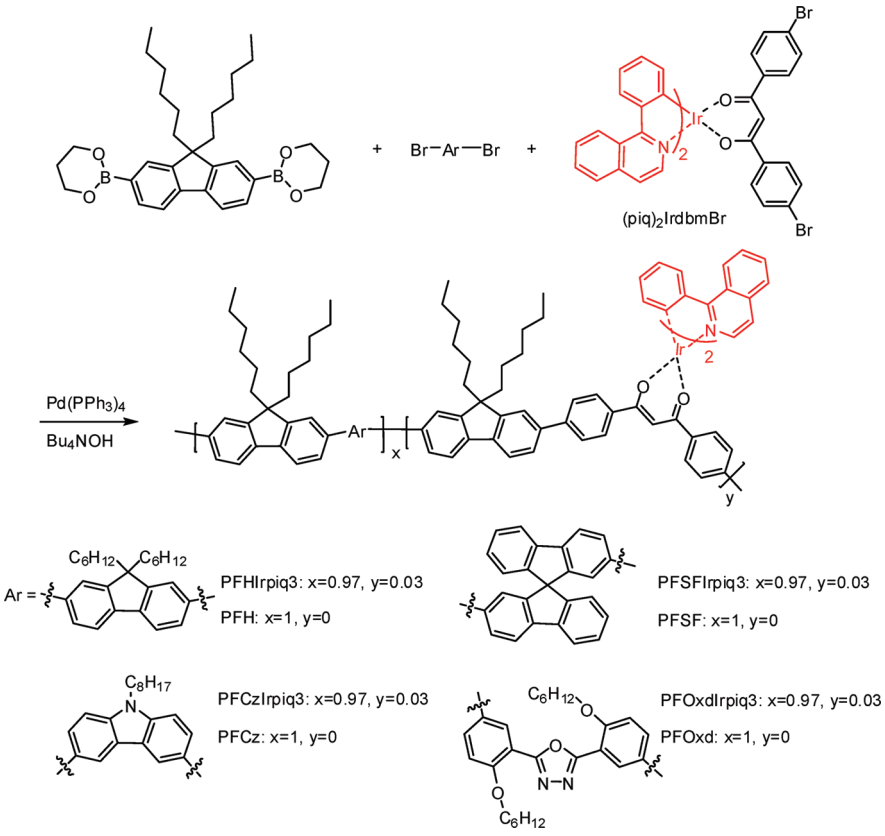

Alfa Step 500 surface profiler (Tencor). A thin layer of Ba (4−5 nm) and subsequently 200 nm layer of Al were vacuum-evaporated subsequently on the top of an EL polymer layer in a vacuum of 1×10^{-4} Pa. Device performances were measured inside drybox. Current−voltage ($I-V$) characteristics were recorded with a Keithley 236 source meter. EL spectra were obtained by Oriel Instaspec IV CCD spectrograph. Luminance external quantum efficiencies were determined by a Si photodiode with calibration in an integrating sphere (IS080, Labsphere).

Results and Discussion

Synthesis and Characterization. The monomers of 2,2′-dibromo-9,9′-spirobifluorene[10] and 2,5-bis-(5-bromo-2-hexyloxy-phenyl)- [1,3,4]oxadiazole[11] were prepared as shown in Scheme 1. The iridium complexes of $(piq)_2$-IrdbmBr and $(piq)_2$Irdbm were synthesized in two steps as reported before.[9] The copolymers were prepared via Suzuki cross-coupling reactions (see Scheme 2). The iridium complex was attached on the polymer backbone by a prefunctionalization method through the β-diketonate ancillary ligand and spread along the polymer backbone randomly. Alternatively, the macromonomers method reported by Evans et al. is a good way to produce the statistical copolymers containing an even dispersion of the pendant iridium complexes.[7] The feed ratio of iridium complex in each copolymer is 3 mol %. The repeat segments on the main chain of copolymers are homofluorene, fluorene-*alt*-carbazole, fluorene-*alt*-spirobifluorene or fluorene-*alt*-oxadiazole, and the corresponding copolymers are named as PFHIrpiq3, PFCzIrpiq3, PFSFIrpiq3, and PFOxdIrpiq3, respectively. The copolymers were characterized by ^{1}H NMR and ^{13}C NMR. The ^{1}H NMR signal at ca. 6.0 ppm, assigned to the methine proton between the two carbonyl groups on β-diketonate ligand, can be observed in the copolymers, except for PFOxdIrpiq3. The actual contents of the iridium complexes were thus estimated to be 1.3% for PFHIrpiq3, 2.3% for PFCzIrpiq3, and 2.4% for PFSFIrpiq3, respectively. On the basis of GPC, the number-average molecular weights of the copolymers are between 7400 and 10690 g/mol with polydispersity indexes between 1.4 and 2.7 (Table 1). The corresponding parent copolymers without iridium complex were also prepared for comparison, and named as PFH, PFCz, PFSF, and PFOxd, respectively. All copolymers can readily dissolve in common organic solvents, such as chloroform, THF, toluene, etc.

Table 1. Structural and Thermal Data for the Copolymers

	complex content (mol %)					
copolymers	in feed ratio	in polymer[a]	M_n	PDI	T_d (°C)	T_g (°C)
PFHIrpiq3	3	1.3	10 690	2.7	77	396
PFCzIrpiq3	3	2.3	7400	1.4	175	397
PFSFIrpiq3	3	2.4	8027	1.7	241	408
PFOxdIrpiq3	3		10 270	1.4	194	398

[a] Evaluated by ^{1}H NMR.

Thermal Analysis. The thermal properties of the copolymers were investigated by thermal gravimetric analysis (TGA) and differential scanning calorimetry (DSC) (Figure 1 and Table 1). The TGA results indicate that

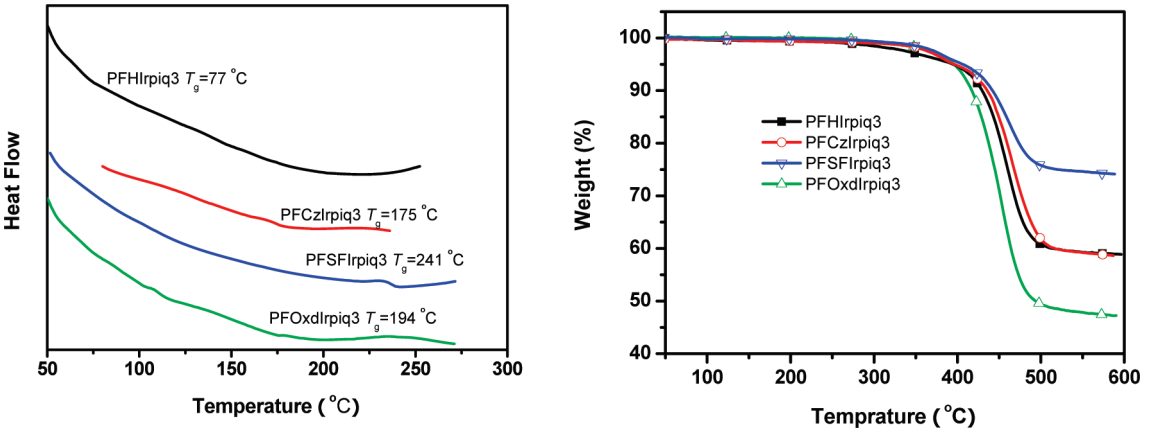

Figure 1. DSC (left) and TGA (right) TGA thermograms of the copolymers.

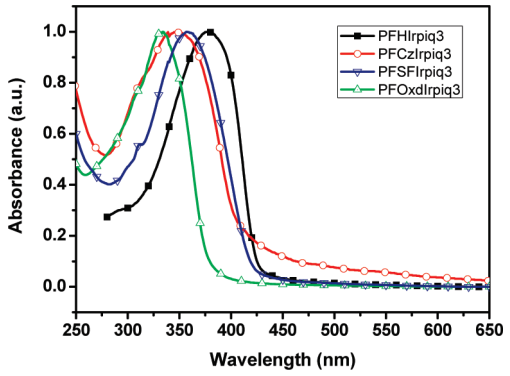

Figure 2. UV−vis absorption spectra of the copolymers in film.

the copolymers have excellent thermal stability with 5% weight loss temperatures from 396 to 408 °C. DSC results reveal that the copolymers are amorphous solids. PFHIrpiq3 with polyfluorene backbone exhibit the same T_g (75 °C) with poly(9,9-dihexylfluorene) (PFH). Contrasting to this, PFCzIrpiq3 and PFOxdIrpiq3 with meta-linked carbazole or oxadiazole segments on main chain show high T_g at 175 and 194 °C, respectively. Furthermore, the T_g is enhanced by 241 °C for PFSFIrpiq3, implicating that the introduction of spirobifluorene units into the backbone significantly improve the morphological stability of the polymer.[13]

Photophysical Properties. The absorption spectra of the copolymers are shown in Figure 2, and the photophysical data are summarized in Table 2. The absorptions of the copolymers are dominated by the corresponding parent copolymers (see Figure S1 in the Supporting Information). With respect to the absorption peak of PFHIrpiq3 at 376 nm, significant blue shifts of 19 nm for PFSFIrpiq3, 27 nm for PFCzIrpiq3, and 36 nm for PFOxdIrpiq3, respectively, were observed. This could be attributed to the interrupted conjugation along the polymer backbone by the meta-linkage (carbazole or oxadiazole) or the sp^3 hybrid carbon (spirobifluorene).[14] The optical energy

Table 2. Photophysical Properties of the Copolymers

	λ_{abs}[a] (nm)	λ_{PL}[a] (nm)	Q_{PL}[b] (%)	E_g[c] (eV)	λ_{EL}[d] (nm)
PFHIrpiq3	376	622	12.0	2.93	626
PFCzIrpiq3	349	624	16.4	3.02	631
PFSFIrpiq3	357	623	20.7	3.00	627
PFOxdIrpiq3	330	626	17.2	3.26	632

[a] Measured in film. [b] Measured in film using PFH as reference. [c] Deduced from the onset absorption. [d] Measured in EL device.

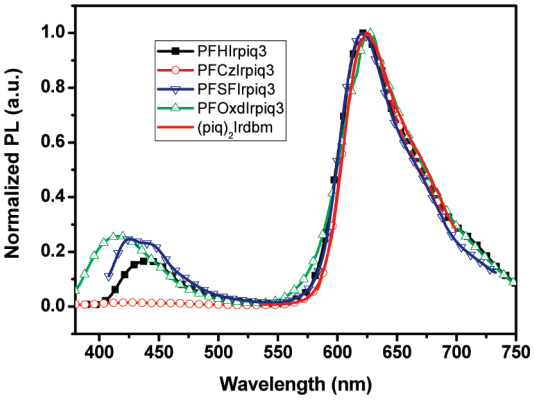

Figure 3. PL spectra of the copolymers in film and $(piq)_2Irdbm$ in CH_2Cl_2.

gaps (E_g) of the copolymers estimated from the onset absorptions follow the sequence of PFOxdIrpiq3 > PFSFIrpiq3≈PFCzIrpiq3 > PFHIrpiq3, which is inverse of the π-electron delocalization degree over the polymer backbone.

The photoluminescence (PL) spectra of the copolymers and the iridium complex $(piq)_2Irdbm$ are shown in Figure 3. The PL spectra of the copolymers are dominated by the emission of iridium complex at ca. 623 nm, without red-shift relative to the emission of iridium complex. This is contrasting to the PL emission of the copolymers with iridium complex conjugated with main chain segments via cyclometalating CN ligands, which usually exhibit remarkable red shifts with respect to their monomeric complexes because of the extended conjugated length in the ligands.[15] The quantum efficiencies

(13) Zhang, K.; Zou, Y.; Xu, X.; Gong, S.; Yang, C.; Qin, J. *Macromol. Rapid Commun.* **2008**, *29*, 1817.
(14) (a) Rothe, C.; Brunner, K.; Bach, I.; Heun, S.; Monkman, A. P. *J. Chem. Phys.* **2005**, *122*, 84706–1. (b) Higuchi, J.; Hayashi, K.; Yagi, M.; Kondo, H. *J. Phys. Chem. A* **2002**, *106*, 8609.
(15) Zhen, H.; Luo, C.; Yang, W.; Song, W.; Du, B.; Jiang, J.; Jiang, C.; Zhang, Y.; Cao, Y. *Macromolecules* **2006**, *39*, 1693.

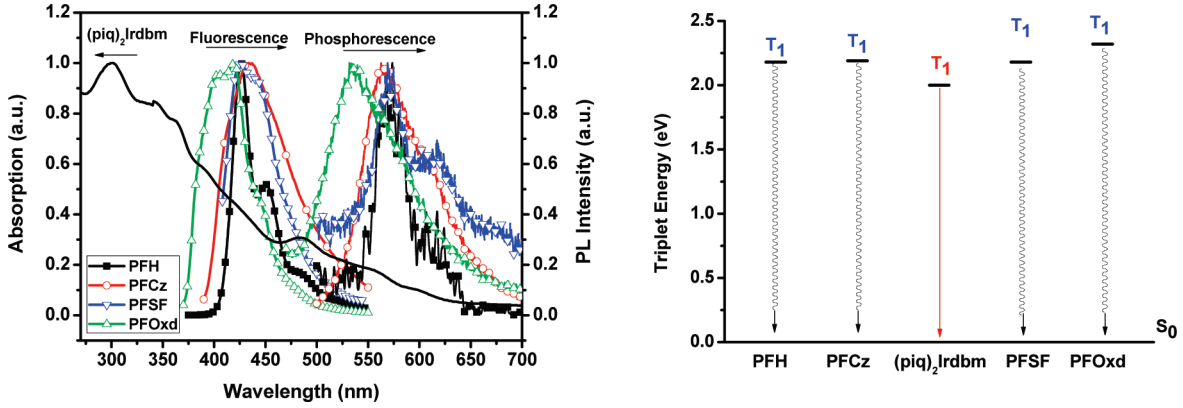

Figure 4. Fluorescence and phosphorescence (measured at 77 K) spectra of parent copolymers in film and absorption spectra of $(piq)_2$Irdbm in dichloromethane solution (left). Schematic triplet energy level diagram of parent polymers and $(piq)_2$Irdbm (right).

Table 3. Electrochemical Data of the Copolymers and the Iridium Complex

	$E_{ox}^{onset\ a}$ (V)	HOMO (eV)	$E_{red}^{onset\ a}$ (V)	LUMO (eV)
PFHIrpiq3	1.00	−5.80	−2.44	−2.36
PFCzIrpiq3	0.78	−5.58		−2.56[b]
PFSFIrpiq3	1.17	−5.97	−2.38	−2.42
PFOxdIrpiq3	1.14	−5.94	−2.33	−2.47
$(piq)_2$Irdbm	0.34[c]	−5.14	−2.18[d]	−2.62

[a] Versus Fc/ Fc^+. [b] Deduced from HOMO and E_g. [c] Measured in CH_2Cl_2 solution. [d] Measured in THF solution.

of the copolymers were measured as film by absolute method using polyfluorene as reference. Compared to PFHIrpiq3 (Q_{PL} = 12%), the other three copolymers show larger quantum efficiencies between 16.4 and 20.7% (Table 2).

To study the singlet and triplet energy transfer between the polymer backbone and iridium complex, we measured the fluorescence and phosphorescence spectra of the parent copolymers, as well as the absorption spectrum of $(piq)_2$Irdbm (Figure 4). The fluorescence emission spectra of the four parent copolymers are similar, with the emission peaks at 427 nm for PFH, 430 nm for PFCz, 425 nm for PFSF, and 420 nm for PFOxd, respectively. The Förster energy transfer from the polymers to the iridium complex is expected to occur because of the good spectral overlap between the emission of the polymers and the absorption of metal to ligand charge-transfer (MLCT) bands (400−520 nm) of the iridium complex. [16] The triplet emission spectra of the copolymers were recorded at low temperature (77 K) upon excitation with 350 nm, and the highest-energy vibronic subbands ($T_1^{v=0} \rightarrow S_1^{v=0}$) were taken as measure for the triplet energy (E_T) of the polymers.[17] The triplet energy of PFOxd (2.32 eV) is significantly higher than those of PFSF (2.18 eV), PFCz (2.18 eV) and PFH (2.10 eV).

Electrochemical Properties. Cyclic voltammetry (CV) was employed to investigate the redox behavior of the chelated copolymers and the iridium complex $(piq)_2$Irdbm (see Figure S2 in the Supporting Information). The electrochemical data are listed in Table 3. On the basis of the low loading of iridium complex in the copolymers, the voltammograms of the chelated copolymers are predominantly characteristics of the corresponding parent polymers. In terms of the onset potentials of the oxidation and reduction, HOMO (highest occupied molecular orbital) and LUMO (lowest unoccupied molecular orbital) energy levels of these materials can be estimated according to the empirical formula $E_{HOMO}/eV = -e(E_{ox} + 4.8)$ and $E_{LUMO}/eV = -e(E_{red} + 4.8)$ with regard to the energy level of ferrocene (4.8 eV below vacuum).[18] The copolymers of

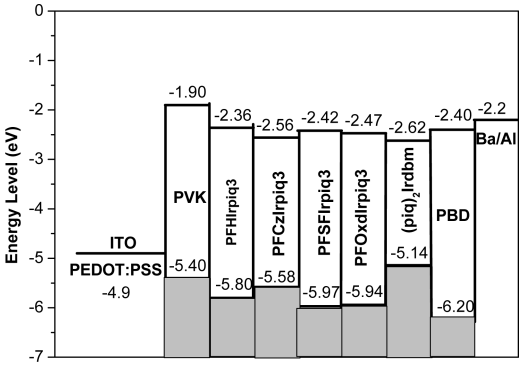

Figure 5. Proposed energy-level diagram with device components.

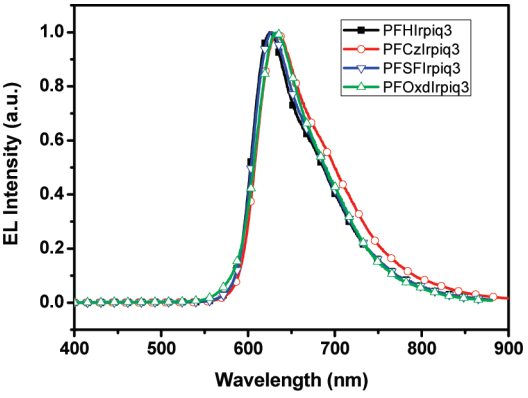

Figure 6. EL spectra of chelated copolymers in device I: ITO/ PEDOT/ copolymer/Ba/Al.

(16) Schimid, B.; Garces, F. O.; Watts, R. J. *Inorg. Chem.* **1994**, *33*, 9.
(17) Dijken, A. V.; Bastiaansen, J. J. A. M.; Kiggen, N. M. M.; Langeveld, B. M. W.; Rothe, C.; Monkman, A. P.; Bach, I.; Stössel, P.; Brunner, K. *J. Am. Chem. Soc.* **2004**, *126*, 7718.
(18) Pommerehne, J.; Vestweber, H.; Guss, W.; Mahrt, R. F.; Baessler, H.; Porsch, M.; Daub, J. *Adv. Mater.* **1995**, *7*, 551.

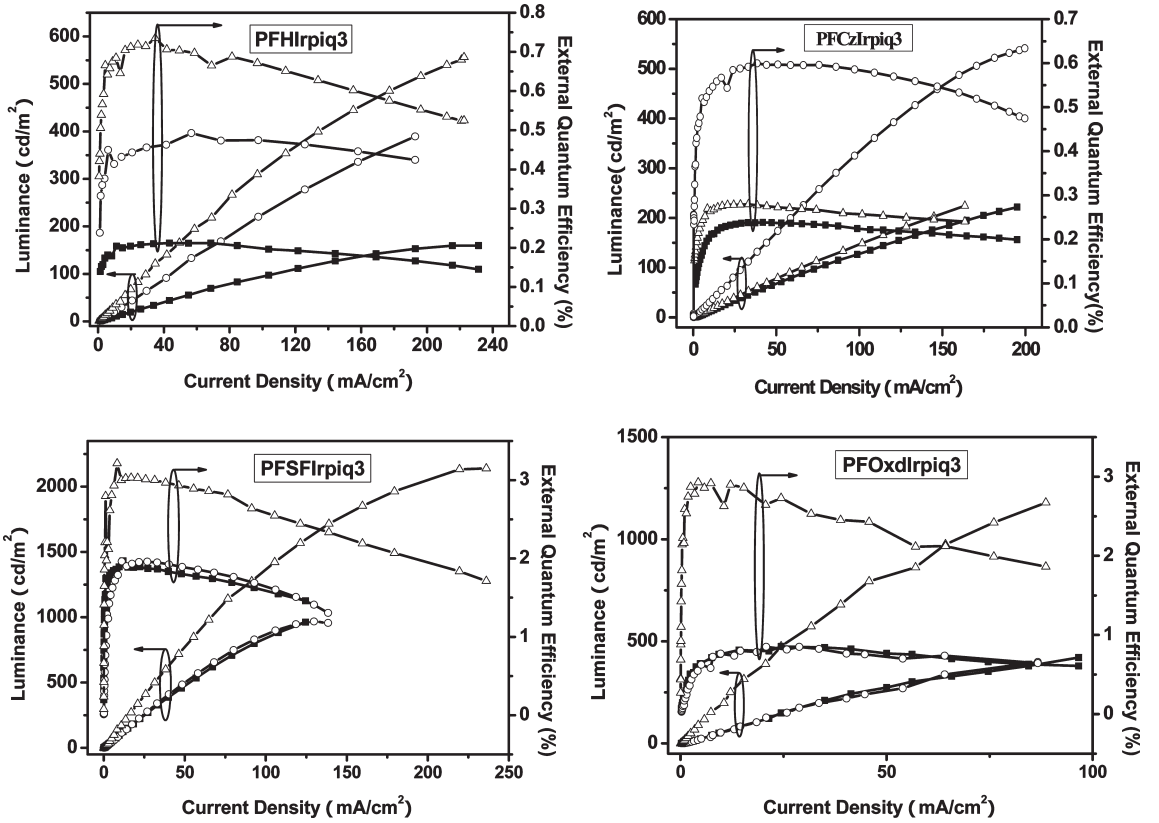

Figure 7. Luminance and external quantum efficiency vs current density for chelated copolymers in device I (diamonds); device II (circle); device III (triangle).

PFHIrpiq3, PFSFIrpiq3, and PFOxdIrpiq3 exhibit reversible or partial reversible oxidation and reduction wave, and their HOMO/LUMO levels are estimated to be −5.80/−2.36 eV for PFHIrpiq3, −5.97/−2.42 eV for PFSFIrpiq3, and −5.94/−2.47 eV for PFOxdIrpiq3, respectively. PFCzIrpiq3 shows partial reversible oxidation wave with onset potential at 0.78 V; however, its reduction potential could not be detected, and thus the difference between the HOMO level (−5.58 eV) and the optical energy gap (E_g = 3.02 eV) was used to estimate its LUMO energy level (−2.56 eV), where E_g was deduced from the onset absorption.

Electroluminescence. We have fabricated three types of PLEDs with the following configurations: device I, ITO/PEDOT (50 nm)/copolymer (80 nm) /Ba (4 nm)/Al (120 nm); device II, ITO/PEDOT (50 nm)/copolymer + 40% PBD (80 nm)/Ba (4 nm)/Al (120 nm); device III, ITO/PEDOT (50 nm)/PVK (40 nm)/copolymer (80 nm)/Ba (4 nm)/Al (120 nm), where an additional PVK layer was used to improve the hole-transport ability and PBD was blended into emitting layer to improve the electron-transport capability as we previously reported (see Figure S3 in the Supporting Information).[3e] In terms of the HOMO/LUMO levels, a band diagram for the device components can be established (Figure 5).

All EL spectra fabricated from the four chelated copolymers exhibit phosphorescent emission peaks around 629 nm originating from the iridium complex, with a little red shifts in comparison with their PL emission maxima (Figure 6). Unlike PL spectra of the copolymer (Figure 3), EL spectra of the copolymers show exclusive triplet emission, and the fluorescence emission from the polymer backbones are completely quenched. This indicates that the charge trapping by iridium complex sites plays an important role under EL excitation except the Förster energy transfer, which is consistent with the fact that the HOMO and LUMO energy levels of $(piq)_2$Irdbm fall within those of the four copolymers.[19]

Figure 7 shows the luminance and external quantum efficiency versus current density for all the devices, and the devices performances are summarized in Table 4.

Compared the different types of devices, we note that the device with PFCzIrpiq3 doped with PBD (device II) showed significantly higher external quantum efficiency than its corresponding devices I and III, whereas the devices with an additional hole-transporting PVK layer (device III) for PFHIrpiq3, PFSFIrpiq3, and PFOxdIrpiq3 exhibited significantly higher external quantum efficiencies than their corresponding devices I and II. (Table 4). The above fact can be elucidated from the different charge-transporting abilities of the copolymers and energy levels of the device components (Figure 5). PFCzIrpiq3 is a hole-transporting material, whereas PBD is an electron-transporting material, and hence doping the latter into the former improved the

(19) (a) Gong, X.; Ostrowski, J. C.; Moses, D.; Bazan, G. C.; Heeger, A. J. *Adv. Funct. Mater.* **2003**, *13*, 439. (b) McGehee, M. D.; Bergstedt, T.; Zhang, C.; Saab, A. P.; O'Regan, M. B.; Bazan, G. C.; Srdanov, V. I.; Heeger, A. J. *Adv. Mater.* **1999**, *11*, 1349. (c) Gong, X.; Lim, S.-H.; Ostrowski, J. C.; Moses, D.; Bardeen, C. J.; Bazan, G. C. *J. Appl. Phys.* **2004**, *95*, 948.

Table 4. Device Performance Data

	PFHIrpiq3			PFCzIrpiq3		
	device I	device II	device III	device I	device II	device III
L_{max} (cd/ m^2)/bias (V) [a]	160/16.0	389/20.0	556/18.7	222/24.0	541/14.8	224/30.0
J (mA/cm^2) [b]	68.6	56.8	34.7	33.0	38.5	33.2
η_{max} (%)	0.21	0.49	0.74	0.24	0.60	0.28
LE_{max} (cd/A)	0.10	0.24	0.35	0.14	0.34	0.16
η at 20 mA/cm^2 (%)	0.20	0.44	0.71	0.23	0.54	0.28
η at 100 mA/cm^2 (%)	0.20	0.48	0.67	0.22	0.59	0.26
η at 100 cd/m^2 (%)	0.20	0.46	0.66	0.23	0.59	0.27
	PFSFIrpiq3			**PFOxdIrpiq3**		
	device I	device II	device III	device I	device II	device III
L_{max} (cd/ m^2)/bias (V) [a]	962/18.4	967/16.3	2140/24.1	420/26.9	399/25.4	1179/30
J (mA/cm^2) [b]	11.9	26.9	8.24	24.5	14.5	4.30
η_{max} (%)	1.97	1.96	3.21	0.85	0.80	2.93
LE_{max} (cd/A)	1.04	1.04	1.70	0.43	0.40	1.46
η at 20 mA/cm^2 (%)	1.89	1.95	3.03	0.80	0.80	2.64
η at 100 mA/cm^2 (%)	1.63	1.60	2.55	0.61	0.64	1.86
η at 100 cd/m^2 (%)	1.89	1.96	2.93	0.80	0.79	2.92

[a] The maximum luminance and corresponding bias. [b] The current intensity for maximum external quantum efficiency and luminance efficiency.

charge-transporting balance, consequently resulting in the great improvement in device efficiency. On the other hand, energy levels of the polymers could affect the balanced charge injection. The HOMO level of PFCzIrpiq3 (−5.58 eV) matches better with the hole-injecting layer PEDOT:PSS (−4.90 eV)[17] than the other three copolymers with a large hole-injecting barrier from 0.9 to 1.07 eV; therefore, adding hole-transporting PVK layer (−5.40 eV) for PFHIrpiq3, PFSFIrpiq3, and PFOxdIrpiq3 decreased the hole-injection barrier, consequently enhancing the device performance.

Comparing the copolymers with different chain configurations, we note that the devices from PFHIrpiq3 and PFCzIrpiq3 exhibit relative poor performance for either device I with external quantum efficiencies around 0.2% or optimized device II and III (lower than 0.8%), whereas the devices from PFOxdIrpiq3 and PFSFIrpiq3 show significantly improved performances. The maximum external quantum efficiencies from PFOxdIrpiq3 is 0.85% for device I, 0.80% for device II, and 2.93% for device III. Noticeably, those values for PFSFIrpiq3 are remarkably enhanced to 1.97% for device I, 1.96% for device II, and 3.21% for device III.

The triplet energy back transfer from iridium complex to the fluorescent polymer has been considered as an important factor for low performance PLEDs for both host−guest blending system[4a] and single phosphorescent copolymer[7].

To explore the nature of the emitting excited states of the chelated polymers and understand the different device performances of the four phosphorescent copolymers, we have measured the decay of PL intensity at 620 nm for the chelated copolymers in thin film, as well as the monomeric iridium complex $Ir(piq)_2dbm$ doped in host PFH for comparison. The decay of the PL intensity at room temperature is fitted to a sum of exponential functions:

$$I(t) = A + B_1\exp(-t/\tau_1) + B_2\exp(-t/\tau_2)$$

The PL lifetime (τ), the relative intensity contributions (B), and goodness of fit (χ^2) are tabulated in Table 5.

Table 5. PL Lifetime of the Copolymers and $Ir(piq)_2dbm$ Doped in PFH

	τ_1 (μs) [a]	B_1 [b]	τ_2 (μs) [a]	B_2 [b]	χ^2 [c]
$(piq)_2Irdbm$/PFH	0.86	0.95			1.07
PFHIrpiq3	0.45	0.87	0.12	0.13	1.03
PFCzIrpiq3	0.35	0.41	0.13	0.59	1.16
PFSFIrpiq3	0.68	0.80	0.21	0.20	1.03
PFOxdIrpiq3	1.31	0.76	0.47	0.24	1.25

[a] Photoluminescence lifetime. [b] Relative intensity contribution. [c] Goodness of fit.

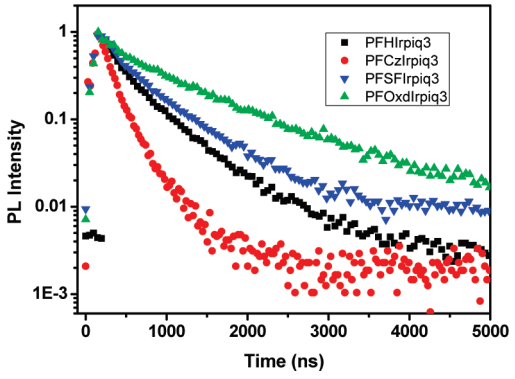

Figure 8. Decay of the PL intensity (excited at 330 nm) at room temperature at 620 nm from thin film of PFHIrpiq3, PFCzIrpiq3, PFSFIrpiq3, and PFOxdIrpiq3.

As shown in Figure 8, the four copolymers show distinct decay characteristics, which can be best described by biexponential fit. This is different from the monoexponential fit of the doping system $(piq)_2Irdbm$/PFH, in which the triplet emission lifetime is mainly determined from the characteristics of the iridium complex. The triplet emission lifetimes of PFHIrpiq3 and PFCzIrpiq3 comprise of long components of 0.45 μs for PFHIrpiq3 and 0.35 μs for PFCzIrpiq3, and short components of 0.12 μs for PFHIrpiq3 and 0.13 μs for PFCzIrpiq3, respectively. The decreased lifetimes of the two copolymers relative to the blending system of monomeric complex and PFH (0.86 μs) are not unexpected because the triplet energy level of the iridium complex (ca. 2.0 eV) is

close to those of PFCz (2.18 eV) and polyfluorene (2.10 eV), and triplet energy back transfer may occur.[20]

PFSFIrpiq3 exhibits a lifetime with a long component of 0.68 μs and a short component of 0.21 μs. Considering the close triplet energy levels of PFSF (2.18 eV), PFH (2.10 eV), and PFCz (2.18 eV), the longer lifetime for PFSFIrpiq3 may mainly be attributed to the orthogonal spirobifluorene segments that can inhibit the aggregation of polymer chains; therefore, the chance for the attached phosphor to be in contact with the main chain is decreased. In other words, the steric hindrance of spirobifluorene suppresses the interchain triplet energy back transfer. This case is similar to shielding the main chain from phosphors with bulky side chain in blending system reported by Chen. et al.[6] In addition, the alleviation of the triplet−triplet annihilation due to the sterically hindered chain configuration should also be responsible for the longer lifetime in PFSFIrpiq3.[21] The longest decay lifetime among the four copolymers with a long component of 1.31 μs and a short component of 0.47 μs is observed for PFOxdIrpiq3. This can be elucidated from its relative high triplet energy level of 2.32 eV, which suppress the intrachain triplet energy back transfer from phosphor to polymer backbone.

Though the triplet lifetime of PFSFIrpiq3 is shorter than that of PFOxdIrpiq3, the EL efficiency for PFSFIrpiq3 is significantly higher than that for PFOxdIrpiq3. This suggests that the triplet energy back transfer could not fully account for the electrophosphorescent efficiency. The PL quantum yields, forward energy transfer from host to guest and morphological stability may also play roles in determining device performance.[6,7]

It is noteworthy that the EL efficiencies using PFOxdIrpiq3 and PFSFIrpiq3 as emitting layer are not only higher than those of analogous phosphorescent polymers with iridium complexes on main chain, but also higher or comparable with those obtained from copolymers with iridium complexes as a pendant group. For example, a maximum external quantum efficiency of 1.29% is achieved from poly(9,9-dihexylfluorene-*alt*-3,4-thiophene) with the green-emitting iridium complex $Ir(ppy)_3$ chelated on main chain;[8] An external quantum efficiency of 2.0% ph/el at 100 cd/m^2 is achieved from poly(9,9-dioctylfluorene) with the red-emitting iridium complex $(btp)_2Ir(acac)$ as side chain via a $-(CH_2)_8-$ spacer.[7]

Conclusions

We have prepared a series of phosphorescent copolymers with a red-emitting iridium complex embedded onto main chain comprised of homofluorene, fluorene-*alt*-carbazole, fluorene-*alt*-spirobifluorene, or fluorene-*alt*-oxadiazole repeat segments, respectively, to systematically investigate the relationship between polymeric electrophosphorescence and polymer chain configurations. We found that the introduction of spirobifluorene units on the backbone significantly reduce the triplet energy back transfer from the attached phosphor to the polymer backbone. The observation suggests a new conception that triplet energy back transfer from an attached phosphor to polymer backbone could be suppressed not only by enhancing the triplet energy (E_T) of polymer backbone but also by introducing a steric hindered units on the backbone to prevent the contact between phosphor and main chain. This provides a new route to design highly efficient electrophosphorescent polymer.

Acknowledgment. We thank the National Natural Science Foundation of China (50773057, 20474047), the Ministry of Science and Technology of China through the 973 program (Grant 2009CB623602), and the Ministry of Education of China for New Century Excellent Talents in University (NCET-04-0682) for financial support.

Supporting Information Available: Absorption spectra of the parent copolymers, cyclic voltammograms of the chelated copolymers and $(piq)_2Irdbm$, and the device configurations (PDF). This material is available free of charge via the Internet at http://pubs.acs.org.

(20) Dorothee, W.; Stephen, P. D.; Stefan, C. J. M.; René, A. J. J. *Chem. Phys. Lett.* **2005**, *411*, 273.
(21) (a) Spehr, T.; Pudzich, R.; Fuhrmann, T.; Salbeck, J. *Org. Electron.* **2003**, *4*, 61. (b) Wong, K. T.; Ku, S. Y.; Chieng, Y. M.; Lin, X. Y.; Hung, Y. Y.; Pu, S. C.; Chou, P. T.; Lee, G. H.; Peng, S. M. *J. Org. Chem.* **2006**, *71*, 456. (c) Natera, J.; Otero, L.; Sereno, L.; Fungo, F.; Wang, N. S.; Tsai, Y. M.; Hwu, T. Y.; Wong, K. T. *Macromolecules* **2007**, *40*, 4456.